Sub-nanosecond delay of light in (Cd,Zn)Te crystals

T. Godde,[1] I. A. Akimov,[1,2,*] D. R. Yakovlev,[1,2] H. Mariette,[3] and M. Bayer[1]

[1] *Experimentelle Physik II, Technische Universität Dortmund, 44221 Dortmund, Germany*
[2] *A.F. Ioffe Physical-Technical Institute, Russian Academy of Sciences, 194021 St. Petersburg, Russia*
[3] *CEA-CNRS group "Nanophysique et Semiconducteurs", Institut Néel, CNRS and Université Joseph Fourier, 25 Avenue des Martyrs, 38042 Grenoble, France*

(Dated: July 13, 2010)

We study excitonic polariton relaxation and propagation in bulk $Cd_{0.82}Zn_{0.12}Te$ using time-resolved photoluminescence and time-of-flight techniques. Propagation of picosecond optical pulses through 745 μm thick crystal results in time delays up to 350 ps, depending on the photon energy. Optical pulses with 150 fs duration become strongly stretched. The spectral dependence of group velocity is consistent with the dispersion of the lower excitonic polariton branch. The lifetimes of excitonic polariton in the upper and lower branches are 1.5 and 3 ns, respectively.

PACS numbers: 71.36.+c / 78.47.D- /78.40.Fy

When the energy of a photon is close to that of an exciton resonance in a semiconductor its group velocity for propagation may be significantly decreased. This phenomenon originates from exciton-photon interaction, which can be considered in terms of an excitonic polariton (EP) quasi-particle[1–3]. The EP propagation and its dispersion have been widely studied using various experimental techniques in different semiconductor materials[1,4–12]. Time-of-flight measurements using pulsed lasers in conjunction with time-resolved detection resulted in group index measurements up to several thousand in GaAs, CuCl and CdSe crystals[4–6]. In some materials like anthracene light may propagate even at velocities below that of sound[7]. Additionally several coherent effects may take place during optical pulse propagation. In linear regime interference between the lower (LP) and upper (UP) polariton branches leads to a beating signal, first observed for the 1S quadrupole exciton in Cu_2O[8]. Nonlinear effects like self-induced transparency at the A-exciton in CdSe and at the bound exciton in CdS have been also studied using frequency-resolved gating[9] and bandwidth limited time-resolved spectroscopy[10], respectively.

Many of the experiments on EP propagation in direct band gap semiconductors like GaAs, CdSe or CdS were performed for resonance conditions on relatively thin crystals (with thicknesses normally below tens of μm)[1,4,6,9,10]. In this case EP in both lower and upper branches propagates through the crystal without significant losses. Although the group velocity is reduced thousand times the optical delay is in the range of several to tens of picoseconds only. It is also known that the EP energy relaxation within the lower branch is strongly suppressed due to the phonon bottleneck in the relaxation path[13]. This effect may be used for long distance coherent EP propagation and realization of long delays for optical pulses. Recently large delays of light in the order of several hundreds of picoseconds were reported in 1 mm thick GaN crystals[12]. Here we report on the direct measurement of sub-nanosecond optical pulse delays in (Cd,Zn)Te crystals which are attributed to propagation of the excitonic polariton in the lower branch. High quality samples with low impurity concentrations result in significant transmission levels in crystals with about 1 mm thickness. The detected group velocity is only 150 times smaller than the speed of light, but the resulting time delay accumulated in the crystal can reach almost half a nanosecond. The effects is pronounced at low temperatures $T \leq 25$ K, but disappears with temperature increase due to enhancement of the EP scattering on acoustical phonons.

In a single oscillator model the dependence of the dielectric function on optical frequency ω and wavevector k is given by

$$\epsilon(\omega, k) = \epsilon_B + \frac{f\omega_0^2}{\omega_0^2 - \omega^2 + (\hbar k^2/M)\omega_0 - i\omega\Gamma}, \quad (1)$$

where ϵ_B is the background dielectric constant, f is the oscillator strength, ω_0 is the resonance frequency, M is the exciton effective mass and Γ is the exciton damping[14]. Solution of $\epsilon = (ck/\omega)^2$ yields the dispersion relation for transversal EP modes, comprising the lower (LP) and upper (UP) polariton branches. Here c is the speed of light in vacuum. Obviously, the single oscillator model gives a simplified description of EP dispersion, especially in zinc-blend crystals like (Cd,Zn)Te where the band structure is complex[15]. However, being mainly interested in the LP branch at optical frequencies $\omega \leq \omega_0$, this simple model gives good agreement with the experimental results. The main parameters for CdTe are known from resonant Brillouin scattering, namely $\epsilon_B = 11.2$, $f = 8.8 \times 10^{-3}$ and $M = 2.4$ in units of the free electron mass[1,16]. The energy dispersion curves for the UP and LP branches are plotted in Fig. 1(a) for $\hbar\omega_0 = 1.6638$ eV, neglecting the damping ($\Gamma = 0$).

The investigated sample was prepared from the ingot of bulk $Cd_{0.88}Zn_{0.12}Te$ crystal grown by Bridgman technique, which corresponds to a growth process at high temperature (1200°C). The crystal was cut along the (100) direction and after chemical-mechanical polishing had a thickness of 745 μm. The crystal had a very good

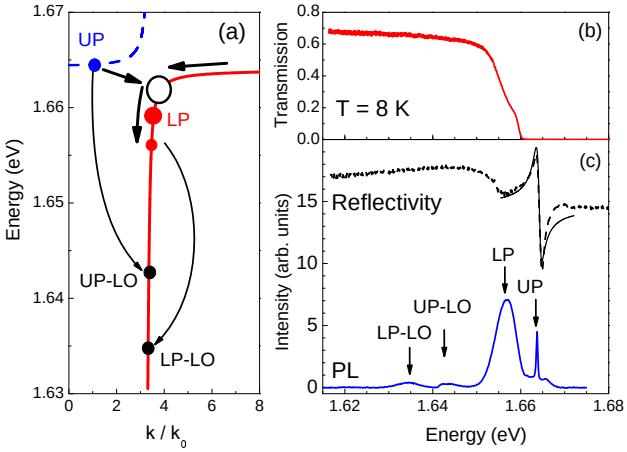

FIG. 1: (a) Excitonic polariton energy-wavevector dispersion ($k_0 = \omega_0/c$). Circles schematically show the EP population, and arrows indicate relaxation paths under non-resonant excitation. (b,c) Steady-state transmission, reflectivity and PL spectra at $T = 8$ K. PL spectrum was taken under non-resonant excitation $\hbar\omega_{exc} = 2.33$ eV at pump power density $P = 100$ mW/cm^2. Solid line is fit of the reflectivity spectrum with $\hbar\omega_0 = 1.6638$ eV and $\Gamma = 1$ meV[17].

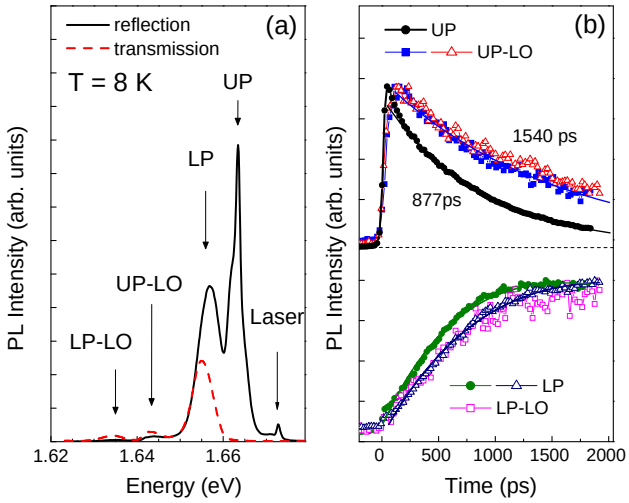

FIG. 2: (a) Time-integrated PL spectra under pulsed excitation with pulse duration τ_D=1 ps and $\hbar\omega_{exc} = 1.673$ eV in reflection (solid line) and transmission (dashed line) geometries. (b) Intensity transients of UP, LP and their LO phonon replicas measured in reflection (full symbols) and transmission (open symbols). Solid lines are exponential fits. The rise time of the UP and UP-LO peaks corresponds to the decay time of the LP peak in reflection and transmission, respectively.

crystalline quality (rocking curve width less than 20 arcsec with an etched pits density 10^4 cm^{-2}). The crystal was not intentionally doped resulting in slightly p-type with a concentration in the order of 10^{15} cm^{-3}.

For time-resolved photoluminescence (PL) and time-of-flight measurements we used a mode-locked Ti:Sa laser. The laser emitted transform limited pulses with 1 ps or 150 fs duration at a repetition frequency of 76 MHz. The sample was mounted in a He-bath cryostat with a variable temperature insert. The PL signal was collected in reflection or transmission geometry. For time-of-flight measurements the optical pulses hit the sample at normal incidence and the transmitted light was detected. The signal was dispersed by a single 0.5 m spectrometer with 6.28 nm/mm linear dispersion and detected with a streak camera. The overall temporal and spectral resolution of the experimental setup for time-resolved measurements was about 20 ps and 1 nm, respectively. For time-integrated measurements a nitrogen cooled charge-coupled-device camera connected to the same spectrometer with 1.3 nm/mm linear dispersion was used. Steady-state reflectivity and transmission measurements were performed using a halogen lamp. For steady-state PL we used a continuous wave laser with $\hbar\omega_{exc} = 2.33$ eV.

Figures 1(b) and 1(c) show low temperature ($T = 8$ K) time-integrated steady state transmission, reflectivity and PL spectra. From reflectivity it follows that the free exciton resonance is located at $\hbar\omega_0 = 1.6638$ eV with $\Gamma = 1$ meV. In the PL spectrum the narrow peak at 1.6637 eV is due to radiative emission from the bottom of the UP branch. Consequently the PL maximum of UP is red shifted by 0.66 meV relative to the expected value $\hbar\omega_0 + \Delta_{LT}$, where $\Delta_{LT} = f\hbar\omega_0/2\epsilon_B = 0.65$ meV is the longitudinal-transversal splitting. This may be result of EP localization on alloy fluctuations[18]. The resulting energy fluctuations are, however, small enough compared to Γ to neglect them. At lower energies we find a broader peak centered around 1.657 eV, which we attribute to emission from the lower EP branch. The LO phonon replica of the UP and LP lines are shifted by $\hbar\omega_{\rm LO}$=22 meV to lower energies. We observe no PL lines related to donor or acceptor bound excitons, which indicates an exclusively pure crystal quality with low background impurity concentration.

PL spectra under pulsed excitation with $\hbar\omega_{exc} = 1.673$ eV in transmission and reflection geometries are shown in Fig. 2(a). It is important to keep in mind that the EP emission occurs only at the crystal surface where the conversion into corresponding photons occurs. The UP branch line is present only in reflection geometry, while the LP peak as well as the phonon replicas of UP and LP are clearly seen in both configurations. This is in accord with the transmission spectrum in Fig. 1(b), i.e. the edge is located just below $\hbar\omega_0$. This indicates that polaritons from the lower branch below the phonon bottleneck [indicated by the open circle in Fig. 1(a)] more likely reach the crystal surface without further scattering. Indeed, if we consider the EP energy relaxation, which is schematically shown in Fig. 1(a), we expect that after the excitation pulse the polaritons in the UP branch either scatter into the LP branch via acoustic phonon emission or recombine radiatively when they are close enough to the surface.

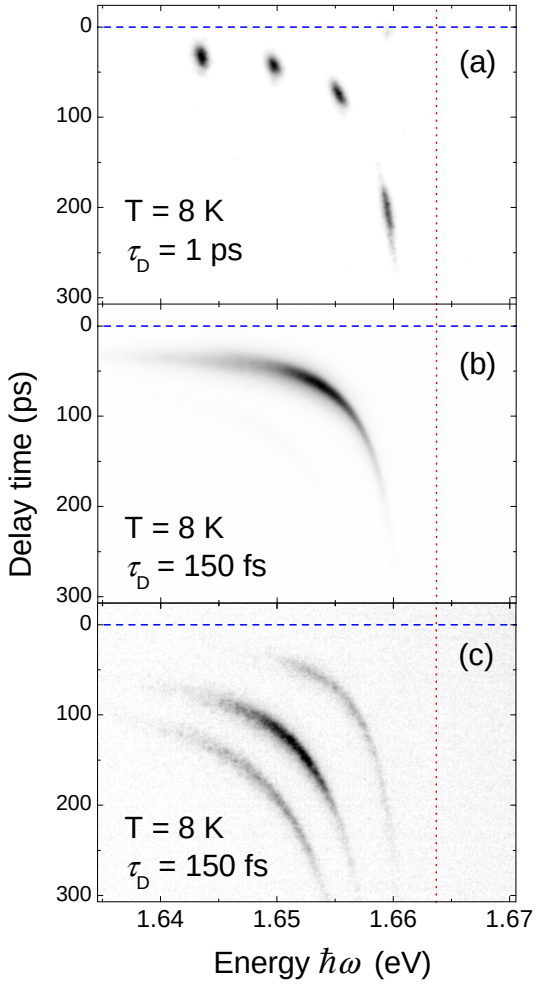

FIG. 3: Grey-scale contour plots of the intensity of the transmitted optical pulse versus delay time and energy for pulse durations of (a) $\tau_D = 1$ ps, (b) and (c) $\tau_D = 150$ fs. In (a) data for four optical pulses with different $\hbar\omega_{exc}$ are superimposed. In order to increase the relative intensity of the replicas in (c) the sample was slightly rotated from normal incidence[21]. Horizontal dashed line indicates zero time, vertical dotted line gives the exciton resonance position $\hbar\omega_0 = 1.6638$ eV.

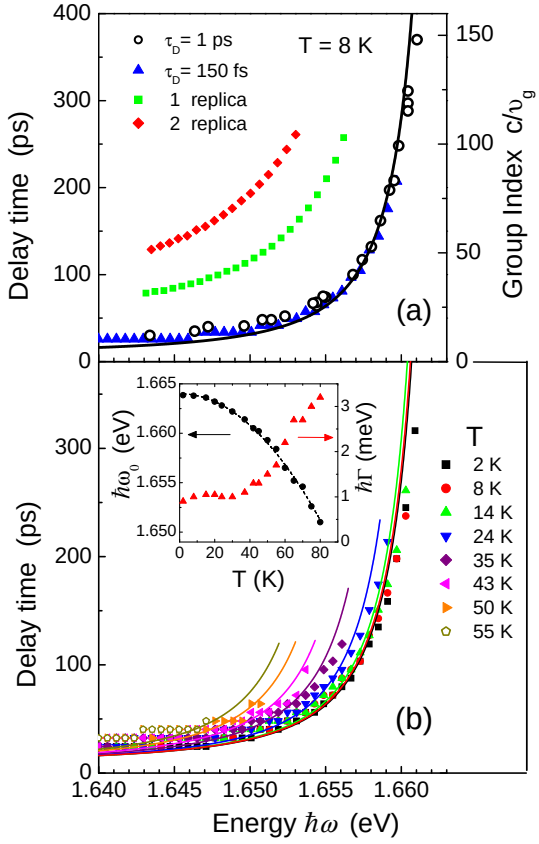

FIG. 4: (a) Delay time/group index as functions of optical pulse photon energy $\hbar\omega_{exc}$ for $\tau_D = 150$ fs (solid triangles) and $\tau_D = 1$ ps (open circles). Solid squares and diamonds represent the delay of the first and second reflection replicas, evaluated from Fig. 3(c). (b) Same as (a) with $\tau_D = 150$ fs for different temperatures. The inset shows the temperature dependence of resonance energy $\hbar\omega_0$ and exciton damping Γ, determined from the reflectivity spectra and used in the group index calculations. Solid lines in (a) and (b) are the delay times calculated with Eqs. (1) and (2).

The remaining EPs gather at the knee of the LP branch, where the probability of acoustic phonon scattering is lowest because of the phonon bottleneck[13]. Finally, they relax further until the group velocity becomes large enough to reach the sample boundary, where they are converted into photons. In case of LO phonon emission the EP always reach the crystal surface and, therefore, LO replicas in the PL spectrum can be used to monitor the corresponding EP dynamics in the sample volume[19].

The transients of UP, LP and their phonon replicas are shown in Fig. 2(b) and confirm the argumentation outlined above. The UP peak in reflection geometry decays with a time of 877 ps, while its LO replica decays with 1540 ps, almost twice longer. The latter corresponds to EP scattering into the LP branch. The decay time of the UP peak may be shorter near the sample boundary due to direct radiative recombination or additional non-radiative recombination at the surface. Note that the UP-LO follows the same dynamics in both reflection and transmission geometries, monitoring the EP kinetics in the sample volume. The LP peak is expected to have a rise time equal to the UP decay time. This is in full agreement with the experimental data. We fit the LP transients in reflection and transmission with double exponential decays where the rise time corresponds to the UP and UP-LO decay, respectively. Good agreement with experiment is obtained for a decay time of about 3 ns, which is attributed to the EP lifetime in the phonon bottleneck region[13,20]. This time constant gives the upper limit for a possible coherent delay of the optical pulse in the LP branch.

After elaborating the EP kinetics we turn now to the results on optical pulse propagation in the LP branch

close to the resonance frequency $\omega \leq \omega_0$. The power density $P \leq 10$ mW/cm^2 was kept low enough to be in the linear regime. The contour plot of the transmitted laser light intensity as function of delay time and photon energy is presented in Fig. 3. In case of spectrally narrow pulses with durations of $\tau_D = 1$ ps a strong dependence of pulse delay on the photon energy $\hbar\omega_{exc}$ is observed, see Fig. 3(a). The delay time increases when $\hbar\omega_{exc}$ approaches the exciton resonance $\hbar\omega_0 = 1.6638$ eV. We were able to observe a maximum delay of 350 ps at $\hbar\omega_{exc} = 1.661$ eV. The transmission of light at this photon energy decreases drastically and is about 0.2% only.

In case of short laser pulses with $\tau_D = 150$ fs strong distortion takes place, see Fig. 3(b). Here, the use of 12 meV spectrally broad pulses centered at 1.653 eV allows one to monitor the EP dispersion in a single measurement. We were also able to detect the subsequent replicas of the pulse, which originate from reflections at both crystal surfaces. The replicas can be seen especially well if the sample is slightly tilted from normal incidence by about 5°, see Fig. 3(c)[21]. As expected, the first and second replicas appear at delays which are respectively 3 and 5 times larger than the delay of the transmitted pulse. In other words the pulses propagate over distances of 3 and 5 times the crystal thickness of 745 μm. We note that we observe no contributions from diffusive propagation, i.e. the photon wavevector is conserved and the pulse propagates through the sample coherently.

It is clear that the spectral dependence of the time-of-flight signal originates from strong variations of the group velocity v_g near the resonance frequency ω_0. In order to quantify the experimental results we summarize the dispersion relations of the group index $n_g = c/v_g$ and the time delay as function of the photon energy for different pulse durations τ_D and temperatures in Fig. 4. As expected, the experimental results are independent of pulse duration, i.e. the dispersion curves for $\tau_D = 1$ ps and 150 fs coincide. The temperature increase leads to a red shift of the dispersion curves. Additionally, the transmission efficiency close to the resonance decreases strongly for temperatures above 25 K.

We calculate the group index according to

$$n_g(\omega) = \frac{c}{v_g(\omega)} = \frac{d}{d\omega}\mathrm{Re}[\omega\sqrt{\epsilon_1(\omega)}], \qquad (2)$$

where $\epsilon_1(\omega)$ is the frequency dependent dielectric function of the LP branch satisfying Eq. (1) and the dispersion equation for transversal modes. The UP branch is not taken into account since the photon energy is below $\hbar\omega_0$. Note that no fitting parameters were used to reproduce the spectral dependence of the group index. As mentioned above, ϵ_B, f and M are known, while ω_0 and Γ are directly taken from the reflectivity measurements at different temperatures, see inset in Fig. 4(b). The results of calculations are shown by the solid lines in Fig. 4 and are in good agreement with the experimental data. The temperature increase leads not only to a red shift of the energy gap, in correspondence with Varshni's law, but also to an increase of damping Γ, as is clearly seen from the inset of Fig. 4(b). The temperature growth of Γ is associated with enhanced EP scattering on acoustical phonons.

In conclusion, we directly observed delays of light pulses up to 350 ps in a 745 μm thick (Cd,Zn)Te crystal. The experimental data are well reproduced using the dispersion relation for the lower EP branch calculated in a single oscillator model. From time-resolved measurements we evaluate lifetimes of EPs in the upper and lower branches of 1.5 and 3 ns, respectively. The realization of large optical delays in ternary alloy crystals like (Cd,Zn)Te is especially attractive as these systems allow control of the resonant frequency over a broad spectral range from 1.6 to 2.4 eV by tailoring the Zn and Cd contents.

The authors are grateful to D. Fröhlich, A.N. Reznitsky and M.M. Glazov for useful discussions.

* Electronic address: ilja.akimov@tu-dortmund.de

[1] E. S. Koteles in *Excitons*, Ch. 3, p. 83, edited by E. I. Rashba and M. D. Sturge (North Holland, Amsterdam, 1982).

[2] S. I. Pekar, Sov. Phys. JETP **6**, 785 (1958) [Zh. Eksp. Teor. Fiz. **33**, 1022 (1957)].

[3] J. J. Hopfield, Phys. Rev. **112**, 1555 (1958).

[4] R. G. Ulbrich, and G. W. Fehrenbach, Phys. Rev. Lett. **43** 963 (1979).

[5] Y. Segawa, Y. Aoyagi, and S. Namba, Solid State Commun. **32**, 229 (1979).

[6] T. Itoh, P. Lavallard, J. Reydellet, and C. Benoit à la Guillaume, Solid State Commun. **37**, 925 (1981).

[7] N. A. Vidmont, A. A. Maksimov, and I. I. Tartakovskii, JETP Lett. **37** 689 (1983) [Pis'ma Zh. Eksp. Teor. Fiz. **37** 578 (1983)].

[8] D. Fröhlich, A. Kulik, B. Uebbing, A. Mysyrowicz, V. Langer, H. Stolz, and W. von der Osten, Phys. Rev. Lett. **67**, 2343 (1991).

[9] N. C. Nielsen, S. Linden, and J. Kuhl, J. Förstner, A. Knorr, S. W. Koch, and H. Giessen, Phys. Rev. B **64** 245202 (2001).

[10] M. Jütte, H. Stolz, and W. von der Osen, J. Opt. Soc. Am. B **13**, 1205 (1996).

[11] B. Sermage, S. Petiot, C. Tanguy, Le Si Dang, and R. André, J. Appl. Phys. **83**, 7903 (1998).

[12] T. V. Shubina, M. M. Glazov, A. A. Toropov, N. A. Gippius, A. Vasson, J. Leymarie, A. Kavokin, A. Usui, J. P. Bergman, G. Pozina, and B. Monemar, Phys. Rev. Lett. **100**, 087402 (2008).

[13] F. Askary and P. Y. Yu, Phys. Rev. B **28**, 6165 (1983).

[14] E. L. Ivchenko in *Excitons*, Ch. 4, p. 141, edited by E. I. Rashba and M. D. Sturge (North Holland, Amsterdam, 1982).

[15] K. Cho, Phys. Rev. B **14**, 4463 (1976).
[16] R. Sooryakumar, M. Cardona, and J. C. Merle, Solid State Commun. **48**, 581 (1983).
[17] $R = |(1-\bar{n})/(1+\bar{n})|^2$, $\bar{n} = (\sqrt{\epsilon_1\epsilon_2} + \epsilon_B)/(\sqrt{\epsilon_1} + \sqrt{\epsilon_2})$, where $\epsilon_1(\omega)$ and $\epsilon_2(\omega)$ are the frequency dependencies of the dielectric functions corresponding to the LP and UP branches, respectively[14].
[18] S. Permogorov, and A. Reznitsky, J. Lumin. **52**, 201 (1992).
[19] E. Gross, S. Permogorov, and B. Razbirin, J. Phys. Chem. Solids **27**, 1647 (1966).
[20] D. E. Cooper and P. R. Newman, Phys. Rev. B **39**, 7431 (1989).
[21] Deviation from normal incidence leads to a slight shift of the reflected beams with respect to the optical axis. This allows one to increase the relative intensity of the corresponding replicas by use of spatially selective detection.